# ON-LINE ARRIVAL TIME AND JITTER MEASUREMENTS USING ELECTRO-OPTICAL SPECTRAL DECODING

Nino Čutić†, Filip Lindau, Sverker Werin, MAX-lab, Lund
Erik Mansten, Department of Physics, Lund University, Sweden

*Abstract*

Electro-optical spectral decoding was used to on-line monitor the arrival time of the electron bunches relative to the seed laser pulse at the test FEL facility at MAX-lab. An infrared chirped pulse coming from the seed laser is influenced by an electron bunch induced birefringence in a ZnTe birefringent crystal and the arrival time is determined from its spectrum. The possibility of running simultaneously with the FEL allowed for a feedback scheme to be built to compensate for the long term drifts in the system. Also, the whole system (the accelerator and the lasers) were synchronized to the power grid frequency. This lock increased the stability and was monitored by the EO setup. Measurements of the bunch length were performed and their correlation with arrival time pointed towards main contributors to the jitter in the system.

## INTRODUCTION

The MAX-lab test-FEL recently demonstrated generation of coherent harmonics at 66 nm (circular and linear polarization) 53 nm and 44 nm (linear polarization) combining seeding at 263 nm and relativistic electron bunch from MAX-lab linac using APPLE II type undulators. One of the crucial components of the test-FEL is a device based on electro-optical spectral decoding (EOSD) which allowed on-line monitoring of the bunch compression and the electron bunch arrival time relative to the seed laser pulse. Since the electron bunch and the seed laser pulse are of subpicosecond duration a technique that allows timing measurements with better precision than what can be achieved with photodiodes ($\sim$200 ps) is needed. Electro-optical schemes using the interaction of a terahertz field created by traveling electron bunch and a laser pulse passing through a crystal have been developed (first in laser based sources of THz radiation) and later modified and applied for measurements of bunch arrival time and duration at accelerators [1, 2, 3]. These technique have shown to be robust enough and comparatively cheap since a required laser pulse for seeded facilities is readily available without major extra costs.

* This work has been partially supported by the EU Commission in the sixth framework program, Contract no. MEST-CT-2005-020356, and the Swedish Research Council.

† Corresponding author; nino.cutic@maxlab.lu.se

## EXPERIMENTAL SETUP

### *The Test-FEL*

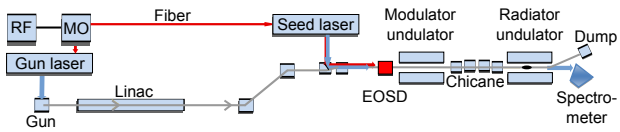


Figure 1: Position of the EOSD within the test-FEL setup. The test-FEL spans about 90 meters in length. The gun laser pulse is used on photo-cathode gun and the seed laser pulse is used for seeding inside the modulator undulator. The master oscillator (MO) is locked to the RF signal generator (3 GHz). Part of the infrared pulse in seed laser is taken and stretched to 3.3 ps FWHM and used for EOSD.

The test-FEL setup is shown in Fig. 1 and consists of 3 major parts [4, 5]. The accelerator (photocathode gun and a recirculating linac, that accelerates 30 pC electron bunches to 375 MeV), the optical klystron (modulator undulator, chicane and radiator undulator) and the laser system (master optical oscillator 93.7 MHz, 790 nm, 13 nm bandwidth, locked to 3 GHz RF clock), two laser amplifiers referred to as the gun laser (263 nm, 10 ps, 10 Hz) and the seed laser (263 nm, 350 fs, 10 Hz, 150 $\mu$J; ) which are positioned in separate laser hutches optically connected by a polarization maintaining fiber that is transferring the oscillator pulse to the seed laser. The energy of the electron bunch is modulated inside the planar modulator undulator due to interaction with the seed laser pulse. It is therefore crucial that the seed laser pulse is transversally and longitudinally (in time) overlapped with the electron bunch, thus the main part of the EOSD system (EOSD chamber) is placed in front of the modulator undulator.

### *The EOSD System*

The EOSD system consists of 3 major parts and operates using a small sample ($<$ 1 $\mu$J) of the amplified seed laser pulse (before it is tripled to UV). The first part of the system is in the seed laser hutch and it consists of a separate stretcher built for IR pulses, focusing optics (telescope focusing onto the crystal inside the EOSD chamber, 6.5 m focus), delay stages (a main delay stage controlling the delay of both pulses relative to the electron bunch, and a UV delay stage shifting the UV pulse relative to the IR pulse) and a UV-IR overlap monitor based on difference frequency generation (DFG). The second part is the EOSD

chamber which is the only part of the EOSD system placed in vacuum. The chamber holds the crystal, a mirror and the photodiode (for rough timing) on a translation stage (used to position the crystal transversally arbitrarily close to the passing electron bunch). The third part is the EOSD detector consisting of the polarization optics and a spectrometer which is placed outside of the vacuum system right next to the chamber. Transverse overlap is controlled by two motorized mirrors before the seed laser pulse enters the vacuum system and it is monitored using two YAG screens positioned before and after the modulator undulator. IR (for EO) and UV (for seeding) pulse are pointing in slightly different directions so that the IR pulse passes through the crystal and hits the mirror behind the crystal (that sends it out of the EOSD chamber into EOSD detector) while UV pulse passes next to the crystal and overlaps with the electron bunch. There is also a slight difference in focusing since the UV pulse is focused in the middle of the modulator undulator.

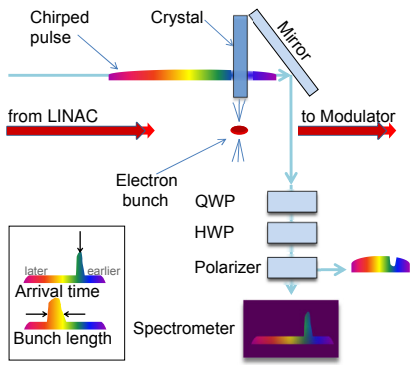


Figure 2: The EOSD chamber and detector. The crystal and the mirror are placed inside the vacuum system on a translatable stage. IR chirped pulse passes through the crystal and is reflected out of the chamber to the detector. The detector consists of polarization optics (Quarter-wave plate, half-wave plate and Glan-laser polarizer) which filters the polarization of interest and the spectrometer. Based on the position of the peak in the signal on spectrometer it is possible to determine the arrival time of the electron bunches relative to the IR pulse and estimate the length of the electron bunch from the width.

Figure 2 shows what is described as the EOSD chamber and EOSD detector. A linearly polarized chirped (3.3 ps FWHM, 5 nm FWHM bandwidth, 790 nm central wavelength) pulse from the seed laser passes through a ZnTe crystal (cut in (110) plane, $5 \cdot 5$ mm$^2$, 1 mm thickness, with [-110] axis pointing up in the figure). The electric field from the electron bunch induces birefringence in the crystal and the crystal changes polarization of the part of the chirped pulse that is currently passing through it. The pulse hits the mirror after the crystal and leaves the vacuum system going into the detector. A quarter-wave plate (QWP) is used to eliminate any residual birefringence in the crystal when there are no electrons present. The half-wave plate (HWP) rotates the polarization of the pulse to the S-polarization of the grating of spectrometer that follows.[1] The pulse passes through the Glan-laser polarizer that filters only the polarization that is not supposed to be present in the pulse (if there are no electrons). The pulse is then sent to the spectrometer. The spectrometer is built using Al-holographic grating 1200 mm$^{-1}$ with Pointgrey Firefly MV camera.

### *Image Analysis*

The images captured by the spectrometer's camera are used to determine the timing of the electrons relative to the UV pulse (since the IR and UV have a fixed delay). The images are median filtered and dead pixels (determined as 1% highest value pixels in dark frame) are attributed the median value of their neighboring pixels. The background spectrum (present without electrons) is subtracted. All pixels in a region of interest are vertically summed and thus resulting curve is considered as signal. Calibration of the pixels to time is done using the signal from electrons themselves and scanning the delay stage that controls the delay of the laser pulse relative to the electrons. This effectively "walks" the peak over pixel values. A polynomial of second order is then used to determine timing of each pixel. A polynomial of second order is used because the chirp of the laser pulse (current frequency along the duration of the pulse) is slightly non-linear. This calibration is repeated several times to remove the contribution from drifts during the calibration itself.

### *Feedback*

To stabilize the drifts a feedback routine is built that controls the position of the peak of the signal so that it is always on desired position (the laser pulse is at desired timing relative to the electrons). This is done by controlling the main delay stage (Thorlabs 150 mm). The routine uses a PI controller whose input is the pixel value of the peak of the signal and parameters are determined using Ziegler-Nichols method. The PI is not compensating on every shot but responds slower after every n shots; this is usually 16 or 8 shots, where the repetition rate is 2 Hz. The change of the delay stage position is suppressed if the required change is less than what would correspond to 30 fs shift in time.

### *50 Hz Lock*

To reduce jitter caused by the 50 Hz grid frequency, the triggering of devices should be synchronized to this frequency. The synchronization is done by a microcontroller sending a trigger pulse every 5 grid cycles to obtain the desired 10 Hz pulse rate. The grid AC is transformed down to

[1] Actually, HWP is offset by about $\sim 1^\circ$ so that even when no electrons are passing the spectrometer can notice the background spectrum of the laser pulse. This is called near-crossed polarizer setup and has certain advantages.

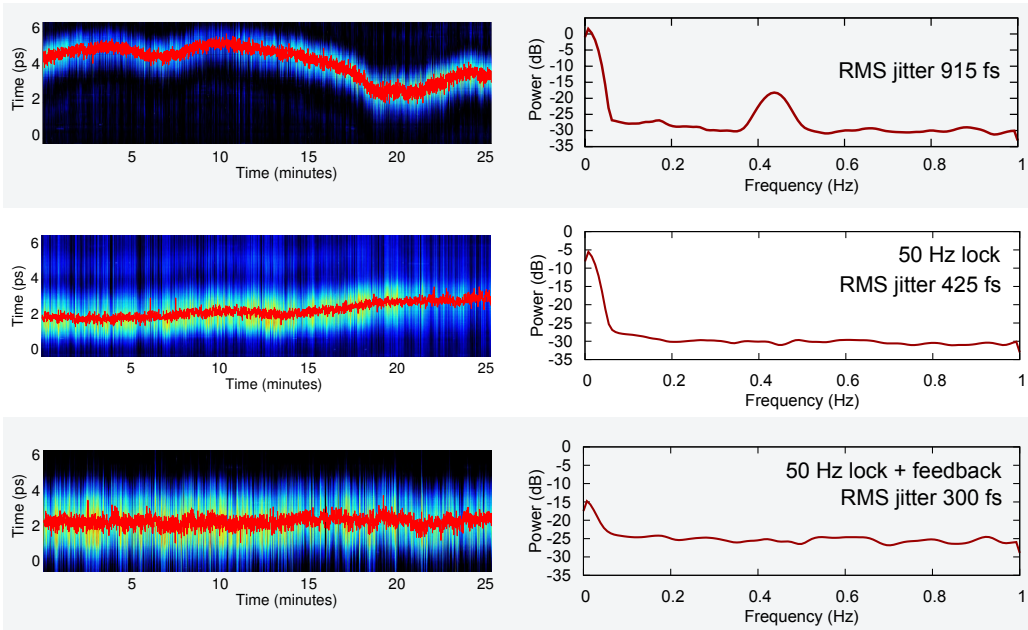


Figure 3: Measurements of the long term drifts and jitter (left) and the corresponding power spectra of the arrival time (right). On the left side each spectrum captured (about 3300 of them, corresponding to 25 minutes) is converted to time and shown vertically using the false coloring of the signal's intensity. The central position is calculated and shown in red overlaid curve. The right side shows power spectra of these red curves. Top - without feedback; middle - with 50 Hz lock; bottom - with EOSD feedback and 50 Hz lock. The RMS jitter drops respectively from 915 fs to 425 fs to 300 fs.

12 V and connected to a comparator input of the microcontroller. When the voltage reaches a set value, an interrupt is generated. To eliminate spurious response around the set value, the microcontroller inhibits the comparator for 16 ms after the first detected crossing.

The trig pulse output from the microcontroller is connected to the trig input of the main delay/trigg generator of the FEL, a Masterclock from Thales Laser, ensuring that the whole system is synchronized to 50 Hz. A jitter of a few tens of microseconds, i.e. less than a degree, has been measured on the 10 Hz trig compared to the grid frequency, mostly due to high frequency components overlaid the 50 Hz signal (from e.g. RF noise). Heavy low-pass filtering would reduce this jitter, but the additional gain in system stability would be minimal.

## MEASUREMENT AND RESULTS

### *Jitter Measurements and Feedback*

The first measurements of jitter were done without the feedback and the 50 Hz lock. Figure 3 on left shows three images each showing a series of spectra through time. A spectrum from spectrometer is shown vertically and converted to time using the calibration polynomial. All three measurements last 25 minutes. Overlaid red line shows the center of each shot. Figures on the right show a power spectrum of the overlaid line determined by using the function *msspectrum* in MATLAB software. The frequencies on the right span to 1 Hz because the repetition (sampling) frequency is 2 Hz. The top two images belong to measurement done without any feedback. The middle two are with the 50 Hz lock is active. And the lower two are with 50 Hz lock active and a PI controller controlling the position of the peak at certain point. Noticeable improvement in stability is visible. Turning on the 50 Hz lock reduces the RMS jitter from 915 fs to 425 fs. It also removes the 0.45 Hz peak which was an influence of the power grid to the system probably on higher frequencies that was undersampled. This still leaves majority of long term drifts below 0.05 Hz which are lowered 10 dB more by the delay stage feedback giving final RMS jitter of 300 fs

### *Drifts and Bunch Length*

Measurements of the bunch length are done simply by determining the width of the EOSD signal. Their main limitation is the large thickness of the ZnTe crystal. Larger thickness of the crystal influences the effective cutoff frequencies of the system (makes the EOSD "slower" due to mismatch between the propagation of the THz and optical pulses through the crystal) but improves the signal strength (larger thickness means more polarization rotation).

Figure 4 shows the correlation between the measured pulse width and arrival time for the case without any feedbacks (overlaid red curve from top left in Fig. 3). Assuming the Gaussian shape of the bunch, simulations show that our setup overestimates the real bunch length by 6% for shorter measurements (1 ps) and 3% for longer (implying the bunch width to be ranging from 0.95 ps to 1.26 ps

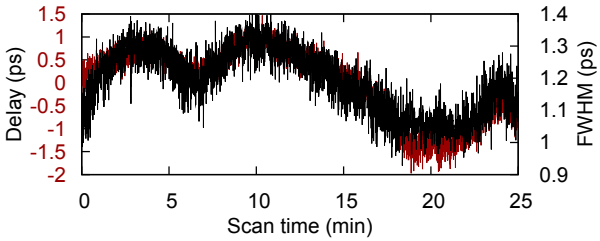


Figure 4: Correlation between the arrival time of electron bunches and the width of the EOSD signal (approximately bunch length, see text). This correlation points to the accelerator as the main cause of drifts.

FWHM). Obvious correlation between the arrival time of electrons and their compression is a sign that the drifts are coming from the linac and not the laser system. If the laser system was the main cause of drifts the compression would not correlate so good with the drifts. During these measurements no automatic control of the compression was used (this requires further work on accelerator side) and is mainly due to hardware contraints.

## CONCLUSION

We used electro-optical spectral decoding to online monitor the compression and arrival time of the electrons relative to the seed laser pulse. A lock to grid frequency and feedback controlling the arrival pulse allowed the reduction of the RMS jitter from 915 fs to 300 fs. These improved conditions were sufficient to achieve the coherent harmonic generation in every shot which effectively increased the signal to noise on the detection side and allowed measurement of lower harmonics (53 and 44 nm). Drift compensation was done controlling the seed laser pulses although the main cause of the drifts comes from instabilities of the accelerator which was determined by observing the correlation between the electron bunch arrival time and the bunch length.

## ACKNOWLEDGEMENTS

Authors acknowledge the use of some of the MATLAB routines to simulate the EOSD developed by Dr. Bernd Steffen which were further modified to estimate the real bunch length from the measured width.

## REFERENCES

[1] I. Wilke, A. M. MacLeod, W. A. Gillespie, G. Berden, G. M. H. Knippels and A. F. G. van der Meer, "Single-Shot Electron-Beam Bunch Length Measurements", Phys. Rev. Lett. **88**, 124801 (2002). doi:10.1103/PhysRevLett.88.124801

[2] T. Tsang, V. Castillo, R. Larsen, Lazarus D. M., D. Nikas, C. Ozben, "Electro-optical measurements of picosecond bunch length of a 45 MeV electron beam", J. Appl. Phys. **89** 4921 (2001). doi:10.1063/1.1358322

[3] B. Steffen, PhD thesis "Electro-Optic Methods for Longitudinal Bunch Length Diagnostics at FLASH", (2007).

[4] S. Werin, J. Bahrdt, N. Čutić, C. Erny, K. Holldack, A. L'Huillier, F. Lindau, E. Mansten, S. Thorin, "First Results of Coherent Harmonic Generation at the MAX-Lab test-FEL", Proc. of the FEL10, Malmö, Sweden, WEOA4, 2010.

[5] S. Werin, N. Čutić, F. Lindau, S. Thorin, J. Bahrdt, K. Holldack, "The test-FEL facility at MAX-lab", Proc. of the FEL09, Liverpool, UK, TUPC034, 2009.